Propylene carbonate reexamined: Mode-coupling β scaling without factorization?

J. Wuttke,[1] M. Ohl,[2] M. Goldammer,[1] S. Roth,[1] U. Schneider,[2] P. Lunkenheimer,[2] R. Kahn,[3] B. Ruffĺe,[4] R. Lechner,[4] and M. A. Berg[5]

[1]*Physik-Department E13, Technische Universität München, 85747 Garching, Germany*

[2]*Experimentalphysik V, Universität Augsburg, 86135 Augsburg, Germany*

[3]*Laboratoire Léon Brillouin, Centre d'Études Nucléaires de Saclay, 91191 Gif-sur-Yvette, France*

[4]*BENSC, Hahn-Meitner-Institut, 14109 Berlin, Germany*

[5]*Department of Chemistry and Biochemistry, University of South Carolina, Columbia, South Carolina 29208*

(Received 27 August 1999)

The dynamic susceptibility of propylene carbonate in the moderately viscous regime above T_c is reinvestigated by incoherent neutron and depolarized light scattering, and compared to dielectric loss and solvation response. Depending on the strength of α relaxation, a more or less extended β scaling regime is found. Mode-coupling fits consistently yield $\lambda = 0.72$ and $T_c = 182$ K, although different positions of the susceptibility minimum indicate that not all observables have reached the universal asymptotics.

PACS number(s): 61.25.Em, 64.70.Pf, 61.12.−q, 78.35.+c

I. INTRODUCTION

A. Motivation

The glass transition, an essentially dynamic phenomenon, can be described as the slowing down and eventual freezing of α relaxation. According to mode-coupling (MC) theory [1,2], the physical origin of this process must be sought on a picosecond scale where long-ranged transport starts to evolve from vibrational short-time dynamics.

In the long-time limit, MC theory reproduces the well-established phenomenology of α relaxation. New results are obtained for shorter times. In particular, the theory predicts a change of transport mechanism around a crossover temperature T_c, located in the moderately viscous liquid phase well above the conventional glass transition temperature T_g. On cooling toward T_c, particles spend more and more time being trapped in transient cages; this process, labeled fast β relaxation, is predicted to obey remarkably universal scaling.

In a couple of structural glass formers, MC predictions have been confirmed [3,4] primarily by different scattering techniques [5,6]. More recently, the GHz–THz dynamics also became accessible by dielectric spectroscopy [7,8]. Although results are in accord with the MC scenario, in several cases the data did not fall together with dynamic susceptibilities from scattering experiments [9,10]. This is in conflict with the asymptotic factorization property of MC β relaxation. Recent theoretical developments suggest explanations on the basis of corrections to scaling [11,12] and orientational degrees of freedom [13,14]. For experimental tests, more detailed comparisons of different observables are needed.

In this context, we undertook incoherent neutron and depolarized light scattering measurements, and reanalyzed dielectric loss and solvation response data on propylene carbonate (PC, 4-methyl-1,3-dioxolan-2-on, $C_4O_3H_6$), a fragile glass former ($T_g = 160$ K, $T_m = 218$–223 K) with low molecular weight ($M = 102.1$), which has already been studied by various experimental techniques. A synopsis of available data shall be given in Sec. I C after collecting the essential results of MC theory in Sec. I B.

B. Mode-coupling crossover

In its simplest (''idealized'') formulation, MC theory describes an ergodic-to-nonergodic transition at T_c. On the low-temperature side, the onset of fast β relaxation leads to an anomalous decrease of the Debye-Waller or Lamb-Mößbauer factor,

$$f_q = f_q^c + h_q |\sigma|^{1/2}, \quad \sigma > 0, \tag{1}$$

with a reduced temperature $\sigma = (T_c - T)/T_c$. On the high-temperature side, the time constant of α relaxation diverges with a fractal exponent γ,

$$\tau \propto |\sigma|^{-\gamma}, \quad \sigma < 0. \tag{2}$$

Such a transition has actually been observed in a colloidal suspension [15]. In a structural glass former, singularities (1) and (2) are smeared out because activated hopping processes restore ergodicity [16]. Under these limitations, integral quantities like f_q or τ_α do not allow for decisive tests of theory. Rather, one has to study the full dynamics, as represented by the dynamic susceptibility $\chi_q''(\omega)$, or any other dynamic variable coupling to it.

Stronger predictions are made for the fast β regime: around the minimum between α peak and vibrational excitations, in a temperature range close enough to, but sufficiently above T_c, any susceptibility is expected to reach the same asymptotic limit

$$\chi''(\omega) = \chi_\sigma g_\lambda(\omega/\omega_\sigma), \tag{3}$$

where the scaling function g_λ is fully determined by one single parameter λ [17]. The amplitude and frequency scale of Eq. (3) should become singular on cooling toward T_c,

$$\chi_\sigma \propto |\sigma|^{1/2} \quad \text{and} \quad \omega_\sigma \propto |\sigma|^{1/2a}, \quad \sigma < 0 \tag{4}$$

where the exponent a, just as γ in Eq. (2), is determined by λ.

TABLE I. Exponent parameter λ and crossover temperature T_c of propylene carbonate as determined by different experimental techniques.

Method	Parameter [a]	λ	T_c(K)	Reference
neutron scattering	f_q	–	210	[18]
Brillouin scattering	f_q	–	270±5	[19]
Brillouin scattering	f_q	– [c]	– [c]	[20]
viscosity [f]	τ_α	0.70	196	[48]
same data	τ_α	0.78[b]	188±3	[20]
neutron scattering	τ_α	0.70[b]	180/188	[48,18]
dielectric loss	τ_α	0.78[b]	187[b]	[23]
VH light scattering	$\omega_{\sigma_\pm}$, $\chi_{\sigma_\pm}$	0.78	187±5[d]	[20]
dielectric loss	ω_σ, χ_σ	0.78	187	[9,22,23]
solvation response [e]	t_σ, τ_α	0.78[b]	176	[25]
same data	t_σ, τ_α	0.72[b]	180±2	this work
neutron scattering	ω_σ, χ_σ	0.72	182	this work
VH light scattering	ω_σ, χ_σ	0.72	182	this work

[a] This column indicates whether the MC fit was based on the Debye-Waller factor f_q [Eq. (1)], the α time scale τ_α [Eq. (2)], or the β relaxation parameters ω_σ and χ_σ [Eq. (4)]. The subscript $\sigma_\pm$ indicates that $T<T_c$ data have also been used.

[b] Used as input.

[c] Determination of MC parameters judged unreliable by the original authors.

[d] The value 179±2 K obtained in an alternative analysis using extended MC theory is not directly comparable to the T_c's from idealized theory.

[e] Transient hole burning on *s*-tetrazine in propylene carbonate. Original analysis.

[f] Original data from Ref. [49].

C. Previous studies of propylene carbonate (PO)

Table I summarizes previous studies of fast dynamics in PC. All authors reported at least partial accord with MC predictions. However, not all MC interpretations were consistent with each other. It is an essential result of idealized MC theory that in the asymptotic β regime all dynamic observables show the same spectral distribution and the same temperature dependence. Therefore, one material is characterized by just one λ and one T_c. Some of the T_c's reported for PC are therefore incompatible with MC theory.

As with other materials, early scattering experiments [18,19] concentrated on the square-root singularity of f_q. As in other materials, this singularity is elusive: in Brillouin scattering, data fitting depends on uncontrolled approximations for the memory function [20]. Similarly, in neutron scattering a determination of T_c from Eq. (1) works at best if the full line shape on the $\sigma>0$ side is known from high-resolution spectroscopy [21]. For these reasons, the results $T_c=210$ or 270 K remain isolated.

In comparison, the determination of T_c from viscosity or α-relaxation data works better. However, available data do not allow for an independent determination of λ, and, even for one given value $\lambda=0.70$, results vary between $T_c=180$ and 196 K.

A dynamic susceptibility has been measured first by depolarized light scattering [20], yielding $\lambda=0.78$ and $T_c=187$. These values have shown to be consistent with dielectric loss spectroscopy [9,22,23]. However, a time-domain optical measurement of the solvation response of a solute molecule found a significantly lower T_c if a light scattering value of $\lambda=0.78$ was assumed [24,25].

In Sec. II, we study the fast relaxation regime by neutron scattering. The λ and T_c we obtain differ significantly from results of the other dynamic measurements which motivates us to remeasure some light scattering spectra (Sec. III) and to reanalyze dielectric-loss and solvation-response data (Sec. IV). Only then will all susceptibilities be compared in Sec. V.

II. NEUTRON SCATTERING

A. Experiments

Inelastic, incoherent neutron scattering has been measured on the time-of-flight spectrometers Mibémol at the Laboratoire Léon Brillouin, Saclay, and NEAT at the Hahn-Meitner-Institut, Berlin. On Mibémol, the counter-rotating choppers were operated with 10 000 rpm. With an incident neutron wavelength of $\lambda_i=8.5$ Å, we obtained a resolution (full width at half maximum) of 6.5–9.5 GHz, depending on the angle. At the Berlin reactor, the flux delivered by the undermoderated cold source decreases rather fast for wavelengths beyond 5 or 6 Å; therefore $\lambda_i=5.5$ Å was chosen. With counter-rotating choppers at 20 000 rpm, we achieved nevertheless a resolution of 11–13.5 GHz. Total count rates were of the same order for both instruments; a precise comparison cannot be made because different sample geometries were used.

For the Mibémol experiment, we used an Al hollow cylinder [26] with a 30-mm outer diameter and a sample layer of about 0.1-mm thickness. In this container, the sample crystallized partially during a 190-K scan; at 175 K, as far as one can tell from the elastic structure factor of a predominantly incoherent scatterer, complete or nearly complete crystallization occurred within 2 h. On the other hand, after rapidly cooling from 260 K, it was possible to perform a 2-K scan in the fully amorphous state.

On NEAT, we tried to remeasure the dynamics of the supercooled state below 200 K. To this purpose, we filled the sample into nearly 200 thin capillaries (soda lime, inner diameter 0.2 mm, Hilgenberg). As in other liquids, this packaging proved highly successful; comparison to a vanadium scattering and visual inspection showed that down to 168 K no crystallization occurred. Because the detectors are located at only 250 cm from the sample, the resolution of NEAT is very sensitive to flightpath differences. We therefore abstained from using a hollow cylindrical geometry; instead, we placed the capillaries in a rectangular holder with a 30-mm base length which was then mounted at 45° with respect to the incoming beam. For both experiments, the sample material, 1,2-propylene carbonate (99.7%, Sigma–Aldrich), was loaded under an inert gas.

After converting the raw data to $S(2\theta,\omega)$, they were binned in about 30 angular groups; a nonequidistant frequency binning was imposed by requiring statistic fluctuations to fall below a given mark. Only then was the container scattering subtracted. The absolute intensity scale was taken from the elastic scattering of the Mibémol 2 K scan; for NEAT, detectors were first calibrated to vanadium before the

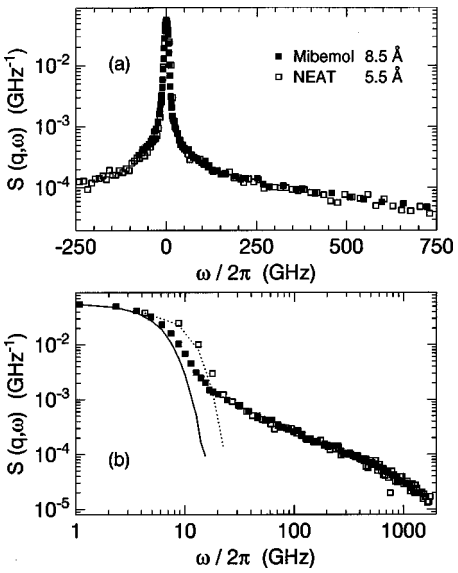

FIG. 1. Incoherent neutron scattering law $S(q,\omega)$ of propylene carbonate at $T=207-210$ K and $q=1.2$ Å^{-1}, measured on two time-of-flight spectrometers under different experimental conditions: Mibémol ($\lambda_i=8.5$ Å, circular Al container) and NEAT ($\lambda_i=5.5$ Å, linear arrangement of glass capillaries). (b) repeats the data of (a) on a double logarithmic scale, and compares them to the measured resolution functions (lines). Above 20 GHz, the quasielastic spectra agree within about statistical error.

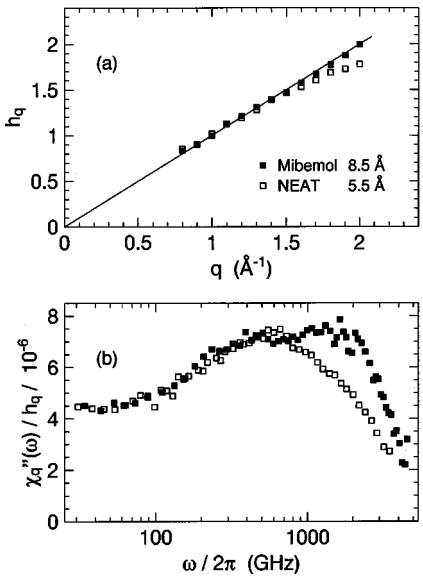

FIG. 2. Decomposition of $\chi_q''(\omega)$ according to factorization (6) for Mibémol (210 K) and NEAT (207 K) data. (a) The amplitude h_q has been determined by least-squares matching between 50 and 2500 GHz. Other methods yield almost identical results. (b) The spectral function $\chi''(\omega)$ is obtained after dividing measured $\chi_q''(\omega)$ by h_q. At low frequencies, the accord between both experiments is excellent; however, at high wave numbers and especially at high frequencies, deviations are strong and systematic. Multiple scattering and imperfect correction for the energy-dependent detector efficiency are probably the main causes for distortions of the spectral line shape.

overall scale was fit to Mibémol at 210 K.

The scattering law $S(2\theta,\omega)$ depends still on λ_i. Only after interpolation to constant wave numbers q one obtains spectra $S(q,\omega)$ which are independent of the kinematics of scattering, and only then a direct comparison between our two experiments becomes possible. This comparison is performed explicitly at 207 and 210 K in Fig. 1. In the quasielastic scattering range, up to some 100 GHz, the accord between Mibémol and NEAT is excellent.

B. Factorization property

For analyzing the data, especially in the quasielastic range, it is advantageous to visualize the scattering law as a susceptibility,

$$\chi_q''(\omega)=S(q,\omega)/n(\omega), \tag{5}$$

with the Bose factor $n(\omega)=(\exp(\hbar\omega/k_BT)-1)^{-1}$.

Around the susceptibility minimum, mode-coupling theory predicts that the β line shape is asymptotically the same for all experimental observables which couple to density fluctuations; thus *a fortiori* it must be the same for incoherent neutron susceptibilities measured at different wave numbers q. We therefore expect $\chi_q''(\omega)$ to factorize into an ω-independent amplitude and a q-independent spectral function:

$$\chi_q''(\omega)=h_q\chi''(\omega). \tag{6}$$

On different theoretical grounds, such a factorization is also expected for incoherent scattering from harmonic vibrations in the lowest order of mass expansion [27,28].

There are several ways to test Eq. (6) and to determine h_q: e.g., one may iteratively construct a model for $\chi''(\omega)$ and fit it to the individual $\chi_q''(\omega)$ data sets. More simply, h_q can be calculated from a least-squares match between neighboring q cuts [28]. For the present data, we find that h_q does not depend on the chosen procedure, nor does it vary with the frequency subrange from which it is determined.

A first surprising result is then the strictly linear wave number dependence of h_q [Fig. 2(a)]. Within MC theory, q dependences can be calculated only if a specific microscopic structure is put in. Within harmonic theory, however, there is a clear expectation that $h_q\propto q^2$. Astonishingly enough, this q^2 dependence is never seen. Instead, in at least two other molecular systems, a linear $h_q\propto q$ dependence is found though the temperature dependence of THz modes indicates pure harmonic behavior [29,30]. From other time-of-flight studies [28,31] we suspect, and a simulation [32] confirms, that this is mainly a multiple-scattering effect. In any case, the linearity is so accurate that in our analysis we shall use Eq. (6) with $h_q=q/q_0$ (with an arbitrary normalization $q_0=1$ Å^{-1}) instead of employing the empirical values.

Figure 3 shows that the factorization holds over the full experimental data range, at least from 30 to 2500 GHz, except for the onset of α relaxation at the highest temperature (which is associated with long-ranged transport, and therefore depends strongly on q). This allows us to condense our huge two-dimensional data sets into q-independent functions $\chi''(\omega)$ with much improved statistics; only on this basis is it possible to proceed with a quantitative analysis of noisy data accumulated in relatively short scans.

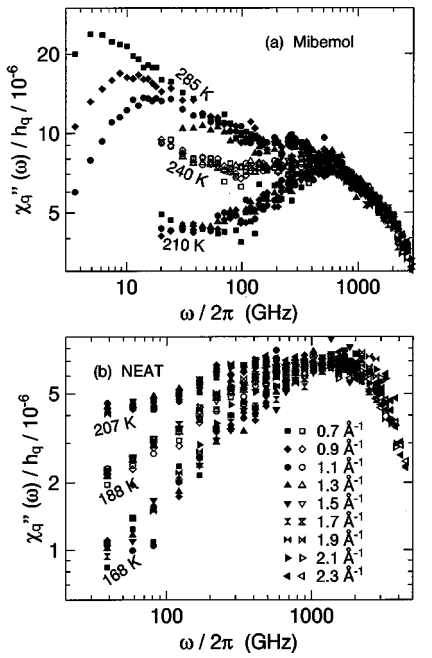

FIG. 3. Rescaled susceptibilities $\chi_q''(\omega)/h_q$. The resolution-broadened elastic line has been cut off, except at 285 K, where the q-dependent α relaxation can be fully resolved. Factorization (6) is confirmed for both the mode-coupling β regime and the vibrational spectra in the THz region.

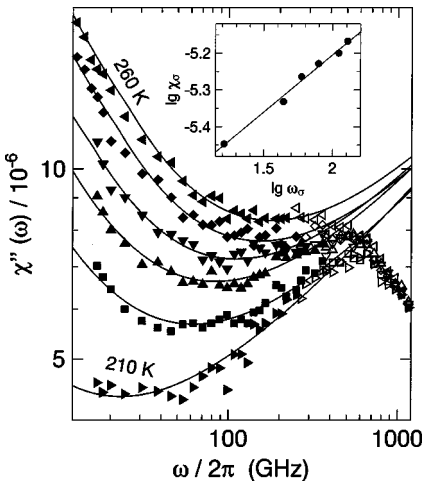

FIG. 4. Susceptibilities $\chi''(\omega)$, obtained as q-independent averages $\chi_q''(\omega)/h_q$ from Mibémol data, for temperatures varying in 10-K steps from 210 to 260 K. Solid lines are fits with the MC asymptote $g_\lambda(\omega/\omega_\sigma)$ [Eq. (3)] with $\lambda=0.72$ fixed. The fit ranges, indicated by full symbols, have been determined in a self-consistent iteration from Fig. 5; at low frequencies, they are limited by resolution or α relaxation, and at high frequencies by the low-lying vibrational peak. In the inset, the logarithms of the fit parameters χ_σ and ω_σ are plotted against each other. The straight line shows the slope $a=0.318$ expected from theory.

Before proceeding with the analysis we have to note that the $\chi''(\omega)$ determined by this method and shown for 207 and 210 K in Fig. 2(b) reveals considerable discrepancies between Mibémol and NEAT at frequencies above about 400 GHz. Although these deviations passed unnoticed on the double logarithmic scale of Fig. 1(b), they are already present in the raw data. While we can exclude container scattering and dark counts as possible causes, two other frequency-dependent effects are likely to contribute: multiple scattering [32] and an inaccurate detector efficiency correction [33]. Multiple scattering cannot be corrected for unless a comprehensive theoretical model of $S(q,\omega)$ is used as input; therefore, it presents a fundamental limitation to the determination of spectral shapes by quasielastic neutron scattering.

C. Master curves for β relaxation

The q-independent $\chi''(\omega)$ can now be used to test the scaling form [Eq. (3)]. We use fits with a fixed λ to determine χ_σ and ω_σ. With these values, a master curve $\chi''(\omega/\omega_\sigma)/\chi_\sigma$ is constructed, and from the master curve a scaling range is read off which is then used for improved fits to the original data. Figure 4 shows fits to the original $\chi''(\omega)$ for $\lambda=0.72$, and Fig. 5 shows master curves for three λ's.

In principle, a self-consistent λ can be determined in an iterative procedure from free fits to the master curves. For our 220–260 K data, λ tends toward values around 0.69 [Fig. 5(a)], but the convergence is erratic, and the outcome depends on a subjective decision of which points to include in the master curve.

With the data on hand, a more restrictive determination of λ is possible from the temperature dependence [Eq. (4)]. The insets in Fig. 5 show that a consistent linear behavior $\chi_\sigma^2 \propto \omega_\sigma^{2a} \propto \sigma$ is found only for $\lambda=0.72$ and $T_c=182$ K; the exponent $a=0.32$, which corresponds to $\lambda=0.72$, is confirmed by cross-checking $\ln\chi_\sigma$ vs $\ln\omega_\sigma$ (inset of Fig. 4).

Figure 5(c) demonstrates that the value $\lambda=0.78$ suggested by preceding light scattering and dielectric loss measurements does not give a good description of the neutron scattering data: the master curve is of poorer quality than for $\lambda=0.69$ or 0.72, especially at frequencies around and below the minimum; free fits with g_λ show a clear trend toward smaller values of λ, and the scales χ_σ and ω_σ do not consistently follow Eq. (4).

At 210 K, the left wing of the susceptibility minimum disappears under the instrumental resolution function, so that a reliable determination of ω_σ is no longer possible. The fit range in Fig. 4 has been chosen such that the resulting ω_σ is consistent with χ_σ. However, the insets in Fig. 5 show that ω_σ^{2a} falls for all values of λ below the mode-coupling expectation (4). Without further experiments, we cannot assess the reliability of the 210 K spectra. We even cannot exclude the possibility of partial crystallization. The line *shape* around the minimum has been checked against NEAT data, but this does not guarantee that absolute intensities are correct. A higher value of χ_σ would allow a higher ω_σ, which in turn would better comply with Eq. (4). Therefore, we exclude the 210 K data from the further analysis. The discrepancy between our $\lambda=0.72$ and the value $\lambda=0.78$ from light scattering motivates us to remeasure some light scattering spectra around the susceptibility minimum.

III. LIGHT SCATTERING

A. Previous studies

Light scattering, just like neutron scattering, comprises coherent and incoherent contributions. Since the wavelength

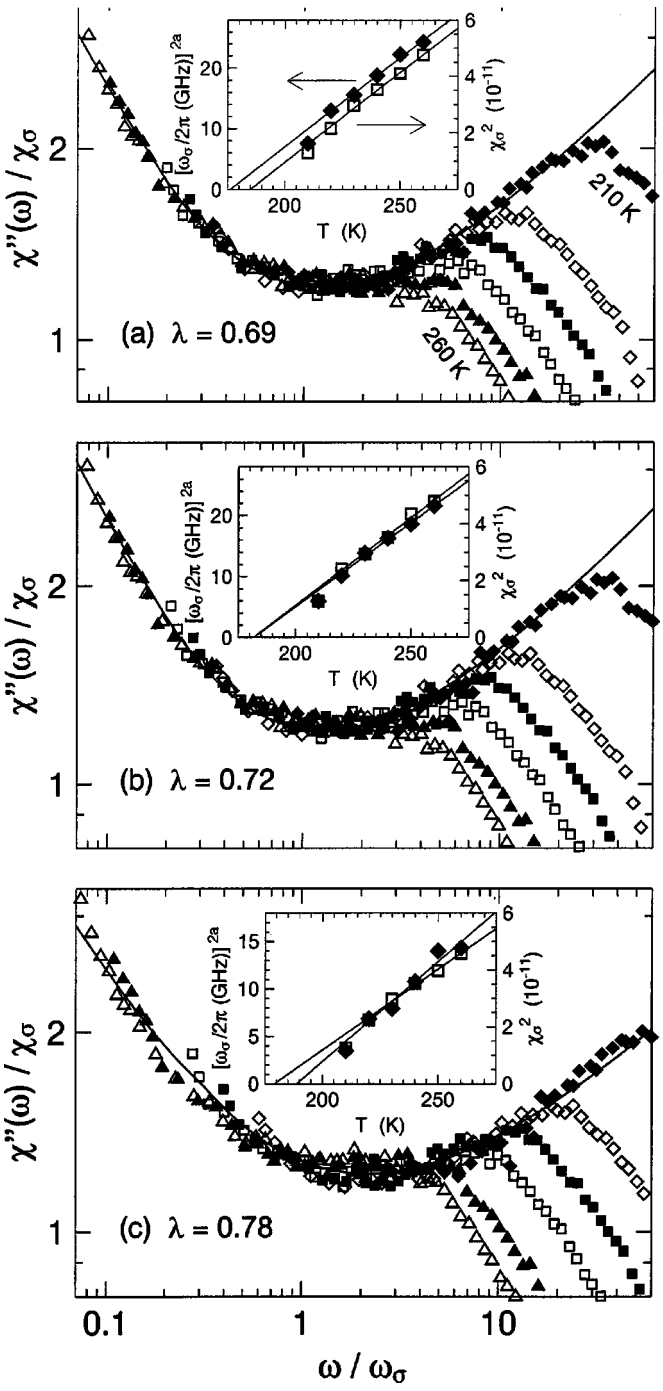

FIG. 5. Susceptibility master curves $\chi''(\omega)/\chi_\sigma$ vs ω/ω_σ from the data set of Fig. 4. Fitting the same original data with different values of λ yields different scales χ_σ and ω_σ, which then lead to distinctly differing master curves. The temperature dependence (4) of χ_σ(□) and ω_σ (◆) is tested in the insets. (a) Iterative rescaling yields a λ of about 0.69 (but unstable and depending much upon idiosyncrasies of the fitting procedure). The temperature dependence of χ_σ and ω_σ is in conflict with (4). (b) For $\lambda \simeq 0.72$, the rescaling is as good as for 0.69, and χ_σ and ω_σ extrapolate from 220–260 K to a consistent $T_c = 182$ K. (c) With $\lambda = 0.78$, as suggested by part of the literature, the master curve is of poorer quality, fits with g_λ show that the imposed value of λ is not self-consistent, and χ_σ and ω_σ are again in conflict with Eq. (4).

of visible light is much longer than molecular dimensions, coherent scattering arises only from sound modes, giving rise to discrete Brillouin lines. Incoherent scattering, on the other hand, ''sees'' local motion and yields a continuous spectrum. In a very first approximation, this spectrum can be interpreted as if it were a q averaged neutron scattering law; microscopic models suggest that the scattering mechanism involves four-point density correlations and/or rotational motion.

Brillouin scattering yields the velocity and damping constant of sound waves. In principle [34], the sound dispersion through the glass transition reveals the strength of the α relaxation so that it is possible to read off the Debye-Waller factor f_q from fits to the Brillouin lines. In practice, this led to an inconsistent estimate of T_c in PC [19]; for a reliable determination of $f_q(T)$, one should not only determine one limiting sound velocity by ultrasonic experiments, but also provide an independently determined memory function as an input [20].

More direct information on the microscopic dynamics is obtained from the incoherent continuous spectra. In order to suppress the much stronger Brillouin lines, these spectra are preferentially gathered in a depolarized (VH) backscattering geometry. In an extensive study of PC, besides a thorough discussion of Brillouin scattering, Du *et al.* [20] also measured VH spectra over a wide frequency band, made accessible by combining a tandem interferometer with a grating monochromator. The measurements extended over a large temperature range, including α relaxation as well as hopping processes below T_c, and were analyzed within both the ''idealized'' and ''extended'' version of MC theory.

While these measurements gave a broad overview of the dynamics of glass-forming PC, they did not yield spectral line shapes with the precision we need now for a quantitative comparison with neutron scattering results. In particular, the exponent parameter $\lambda = 0.78$, obtained within idealized theory from a global fit to $T > T_c$ data, was given with a relatively large error range of ± 0.05. Furthermore, as in other broadband light scattering studies performed until quite recently, the tandem interferometer was used in series with an insufficient bandpass which did not fully suppress higher-order transmissions of the interferometer [35,36]. For these reasons, we remeasured some depolarized spectra, concentrating on the temperature and frequency range of the asymptotic β regime.

B. Experimental setup

Experiments were performed in Garching on a Perot-Fabry six-pass tandem interferometer. The instrument, bought from J. R. Sandercock, was modified in several details to allow for stable operation and high contrast. The six-pass optics was placed in a thermally isolating housing, and the scanning stage was actively temperature stabilized. The analog-electronic stabilization of the interferometer piezos was replaced by computer control. Entrance and exit pinholes were spatially separated from the six-pass optics, so that the most critical alignments could be done without disturbing the interferometer operation. By placing additional masks in the six-pass optics, in particular on mirror surfaces,

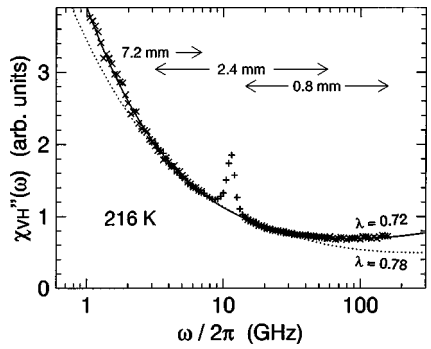

FIG. 6. Susceptibility $\chi_{VH}(\omega)$ from depolarized light scattering from propylene carbonate at 216 K, measured at the Fabry-Perot-Sandercock tandem interferometer at Garching, with $\lambda_i = 514.5$ nm and with mirror spacings $z_0 = 0.8$, 2.4, and 7.2 mm. The matching of the three data sets is excellent, and would extend even further without the VV Brillouin mode leaking around 10 GHz. The solid line is a fit with the MC asymptote $\chi_\sigma g_\lambda(\omega/\omega_\sigma)$, with $\lambda = 0.72$. The dotted line corresponds to the mean literature value $\lambda = 0.78$.

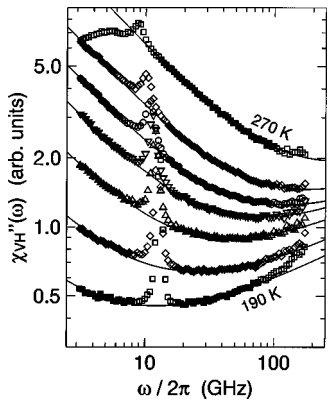

FIG. 7. Depolarized light scattering susceptibilities, combined from two spectral ranges ($z_0 = 0.8$ and 2.4 mm), as functions of temperature. Solid lines are MC fits with fixed $\lambda = 0.72$. Open symbols indicate regions which had to be excluded from the fits: above about 80 GHz there is a crossover to the nonuniversal vibrational spectrum, around 8–15 GHz there is the Brillouin line, and at the highest temperature there is the beginning of α relaxation.

the cross-talk between different passes could be reduced by several orders, and a straylight rejection of better than 10^{11} was achieved.

Depending on the free spectral range, the instrument is used in series with an interference filter of 0.15 or 1 THz bandwidth (Andover); these filters are placed in a special housing with active temperature stabilization. Furthermore, to account for long-term drift, the instrument function is redetermined periodically by automatic white-light scans.

Although the spectrometer guaranteed excellent straylight rejection, special care was taken to prevent direct or diffuse reflections of laser light from entering the instrument. Therefore, instead of 180° backscattering, a 169° VH geometry was chosen. From the intensity transmitted through the ''ghosts'' of the tandem instrument, we conclude that the straylight was about 10^5 times weaker than the inelastic scattering from PC, and completely negligible compared to the detector's dark count rate of about 2.5 sec^{-1}. After subtraction of these dark counts, and normalization to the corresponding white light scans, the resulting spectra showed an excellent detailed balance symmetry. The sample material was from the same source as for the neutron scattering experiment, and was vacuum sealed in a Duran cell.

C. Susceptibilities around ω_σ

For a precise determination of the spectral line shape, subsequent measurements over different spectral ranges were performed after stabilizing the temperature overnight. The most restrictive determination of the exponent parameter was possible at $T = 216$ K. As shown in Fig. 6, the matching of the three overlapping spectral ranges is excellent. Except for the leaking VV Brillouin mode, the VH susceptibility is described over more than two decades by the MC asymptote g_λ. Fits yield $\lambda = 0.72 \pm 0.01$, which is confirmed by measurements at other temperatures as well as by a bulk of earlier experiments we performed under less ideal experimental conditions. This result is at the margin of the error range in the literature value 0.78 ± 0.05 [20]; the figure shows that 0.78 itself is clearly incompatible with our present data.

Second, for two different spectral ranges we measured temperature series. Figure 7 shows some of the composite susceptibilities. From fits with fixed $\lambda = 0.72$, the frequencies ω_σ were obtained. Then the individual susceptibilities, measured around interferometer mirror spacings $z_0 = 0.8$ and 2.4 mm were fitted with fixed λ and ω_σ so that we obtained two independent data sets for the amplitudes χ_σ.

The temperature dependence of ω_σ is shown in Fig. 8(a). Data between 190 and 230 K extrapolate to the same T_c

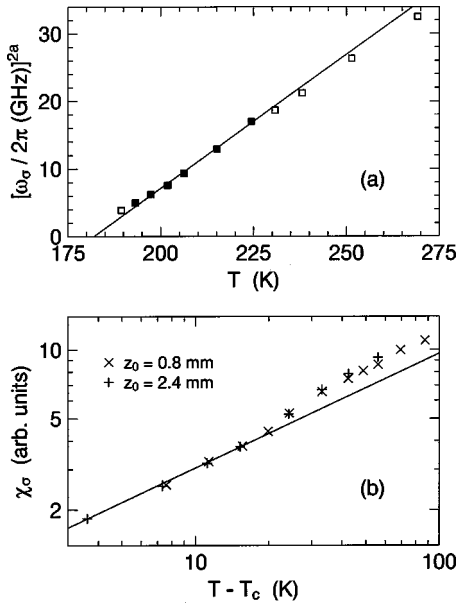

FIG. 8. Scaling parameters obtained from MC fits. The rectified plot (a) confirms that ω_σ evolves with $|\sigma|^{1/2a}$. When fitting only the full symbols, $T_c = 182 \pm 1$ K is obtained in full accord with the neutron scattering result from Fig. 5. When extending the temperature range, T_c tends to decrease by a few K. The amplitudes, determined independently for two spectral ranges, are advantageously represented (b) in a logarithmic plot vs $T - T_c$, with $T_c = 182$ K as determined above. The solid line shows the slope 1/2 expected from theory.

$=182\pm1$ K, as found from neutron scattering. Extending the fit range to higher temperatures leads to a T_c which is about 2 K lower. Again, these results are marginally compatible with $T_c=187\pm5$ K from the earlier light scattering study [20].

Measuring amplitudes in light scattering is difficult, and prediction (4) can be verified only over a reduced temperature range. Results are visualized best in a logarithmic plot of χ_σ vs $T-T_c$ [Fig. 8(b)], which suggests there are two different regions in which χ_σ is proportional to $|\sigma|^{1/2}$, separated by some step. Without further experiments, we must leave open whether this step comes from the sample or presents an experimental artifact, due, for instance, to distortions of the optical paths. We note, however, that after 30 h and a full temperature cycle, we were able to reproduce an amplitude χ_σ within less than 1%. Thus, irregularities in the amplitude are due not to a drift in time, but mainly to reversible effects of temperature variation.

Putting aside the amplitude problem, our results are in excellent accord with the neutron scattering data of Sec. II. This motivates us to reconsider dielectric loss data which were analyzed previously with $\lambda=0.78$.

IV. OTHER SPECTROSCOPIES

A. Dielectric loss

Dielectric spectroscopy on PC was described recently [9,22,23]. The measurements extended over a wide range of temperatures and many decades in frequency, and the analysis addressed different issues which are currently debated in the context of glass transition dynamics.

Within the GHz–THz range, the dielectric susceptibility $\epsilon''(\omega)$ passes through a minimum, as suggested by MC theory. Fits with Eq. (3), approximated as a sum of two power laws [37], gave $\lambda=0.78$, and from the temperature dependence of the frequency and amplitude [Eq. (4)], $T_c\simeq187$ K was found. Though these values had strong support in the existing literature, they differ from our neutron and light scattering results. It is therefore interesting to ask whether the dielectric loss would also allow for $\lambda=0.72$.

Since the available dielectric data are even noisier than the neutron susceptibilities, there is no unique way to determine the scaling range within which Eq. (3) applies; therefore, any value of λ depends on the choice of the fit range. In the previous analysis [23], fits were applied between about 1 and 600 GHz. For temperatures around 200 K this range covered both sides of the minimum equally well. When $\lambda=0.72$ is imposed in an iterative master curve construction, the scaling range escapes toward lower frequencies, as can be seen from the fits in Fig. 9.

For direct comparison, Fig. 10 shows master curves constructed with two different values of λ. In the upper curve, with $\lambda=0.78$, the measured susceptibilities have been rescaled with exactly the ω_σ and ϵ_σ shown in Fig. 8 of Ref. [23]. The rescaling works particularly well on the high-frequency side of the minimum, and nicely shows the ω^a limit which has remained elusive in so many other experimental investigations. The lower curve, constructed with $\lambda=0.72$, shows that the scaling property is completely lost above ω_σ, and that ω_σ is no longer proportional to the minimum position $\omega_{\min}$. On the other hand, the scaling has significantly improved in the low-frequency wing. Furthermore, the ω^{-b} limit of g_λ describes the data nearly up to the α-relaxation maximum where they almost coincide, except for the lowest two temperatures.

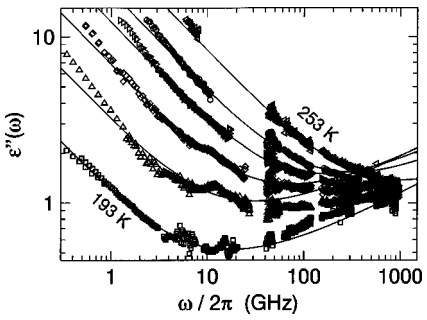

FIG. 9. Dielectric loss data as published in Refs. [9,22,23]. Solid lines are MC fits [Eq. (3)] with fixed $\lambda=0.72$. This figure can be compared directly to Fig. 7 in Refs. [23], where the same data are fitted with $\lambda=0.78$.

This unexpected observation motivates another master curve construction which is quite common in the conventional analysis of α relaxation, but which to our knowledge has never before been applied to MC β relaxation: in Fig. 11, the dielectric data are shown with original amplitude, rescaled only in frequency by the α maximum frequency $\omega_{\max}$. As usual for α relaxation (and in accord with the second scaling law of MC theory) the amplitude and the line shape of the α peak are temperature independent. But here, the scaling behavior extends far down into the high-frequency wing—in fact, it extends as far as the data have been measured, except again the two lowest temperatures, 193 and 203 K.

However, a master curve which extends from the maximum up to the minimum of a dynamic susceptibility cannot simultaneously obey the first and second scaling laws of MC: we expect

$$\omega_{\max}/\omega_{\min}\propto|\sigma|^{1/2b}, \tag{7}$$

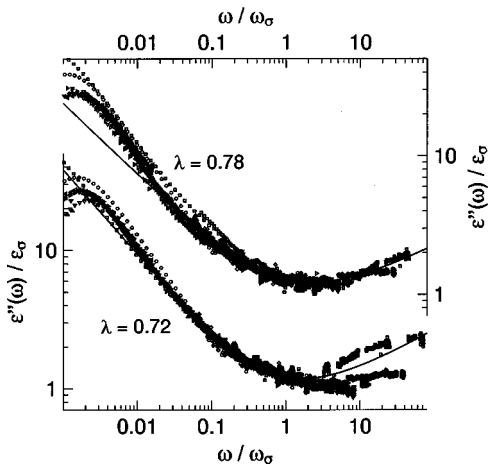

FIG. 10. Dielectric loss data [9,22,23], rescaled to two versions of a master function $\epsilon''(\omega/\omega_\sigma)/\epsilon_\sigma$. In the upper curve, the same ω_σ and ϵ_σ are used as determined in Ref. [23] for $\lambda=0.78$. For the lower curve, $\lambda=0.72$ was imposed, which shifts the scaling range toward the low-frequency wing of the susceptibility minimum.

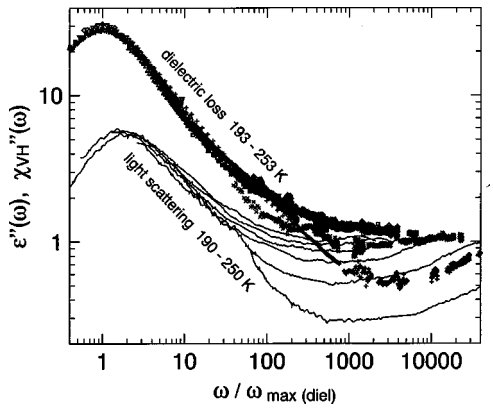

FIG. 11. In this master plot, the frequency scale is taken from the position of the α relaxation peak in dielectric loss, and applied to both dielectric loss $\epsilon''(\omega)$ (same data as in Ref. [23]) and depolarized light scattering $\chi''_{\mathrm{VH}}(\omega)$ (scanned from Ref. [20]). While the $\epsilon''(\omega)$ are shown in absolute units, the amplitude of $\chi''_{\mathrm{VH}}(\omega)$ is arbitrarily rescaled by a global factor so that the microscopic peaks culminate at about equal height. This scaling representation elucidates how a strong α peak reduces the temperature range for which a susceptibility minimum can be observed.

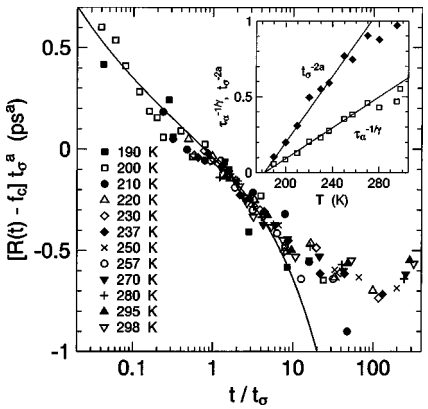

FIG. 12. Solvation response of *s*-tetrazine in propylene carbonate as measured by transient hole burning. Same data as in Fig. 6 of Ref. [25], but now reduced with $\lambda = 0.72$ and $f_c = 0.56$. The solid curve is the scaling function $g_\lambda(t/t_\sigma)$. The deviations at long times are attributed to α relaxation. The inset (cf Fig. 7 of Ref. [25]) shows the temperature scaling of t_σ (t_β in Ref. [25]) and τ_α (both in ps), using the exponents $2a = 0.636$ and $\gamma = 2.395$ that correspond to $\lambda = 0.72$. The fits shown extrapolate to a common $T_c = 182$ K in accord with neutron scattering measurements. (Good fits can be obtained over the range 178–182 K).

and, even more elementary, $\epsilon_{\min} \propto |\sigma|^{1/2}$, whereas $\epsilon_{\max}$ remains constant.

Since there is no doubt about the scaling of α relaxation, we are bound to conclude that the dielectric data do not reach the asymptotic regime of fast β relaxation, except in a rather small temperature range that extends at best to about 210 K. For higher temperatures, the high-frequency wing of α relaxation, though technically describable by g_λ, does not represent the first scaling law limit. This conclusion is independent of any fitting, and does not, in particular, depend upon an imposed value of λ.

B. Solvation dynamics

The solvation response of *s*-tetrazine was measured in PC from 1.5 to 100 ps [24]. A MC analysis in the time domain identified both α- and β-scaling regions in the dynamics [25]. A unified analysis of both regions was consistent with MC theory for a range of λ-T_c pairs. In the original publication, $\lambda = 0.78$ was fixed, in accord with the light scattering analysis of Du *et al.* [20]. However, this value of λ yielded a crossover temperature $T_c = 176$ K substantially below the value obtained by Du *et al.* ($T_c = 187$ K).

The solvation data were reanalyzed by the same method used in Ref. [25], but using $\lambda = 0.72$. The analysis of the α-scaling region is unchanged. Figure 12 shows the new β scaling plot and the fit to $g_\lambda(t/t_\sigma)$, both of which are as good as in the previous analysis. The inset shows a temperature scaling plot of t_σ and τ_α. As expected, the scaling law deteriorates at temperatures far above T_c. Depending on the range of temperatures fit, acceptable values of T_c lie in the range 178–182 K. Thus, the solvation response is consistent with both the λ and T_c obtained in Secs. II and III by neutron and light scattering.

V. COMPARISON OF DYNAMIC OBSERVABLES

A. Direct comparison of susceptibilities

Neutron scattering, light scattering with or without proper bandpass, and dielectric loss: each experiment, taken alone, seemed in full accord with the asymptotic predictions of MC theory. Taken together, the situation becomes more complicated.

In the fast β regime, any observable that couples to density fluctuations is expected to tend toward the same asymptotic limit [Eq. (3)]. For neutron scattering, this prediction takes the form of a q,ω factorization, and is confirmed, in PC as in other materials, over a wide frequency range. However, it breaks down completely when depolarized light scattering or dielectric loss are included.

In Fig. 13, dynamic susceptibilities from neutron scattering, light scattering [38], and dielectric loss are shown for direct comparison on an arbitrary intensity scale, but in absolute frequency units. The result is in flagrant contradiction

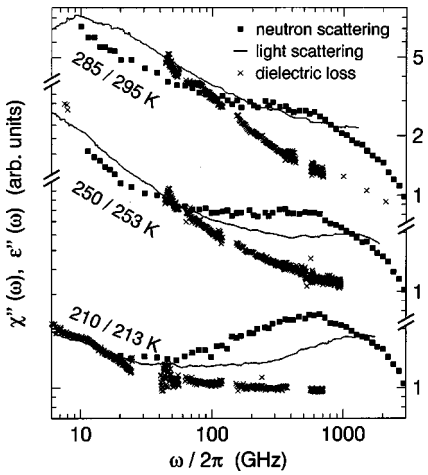

FIG. 13. Direct comparison of susceptibilities from neutron scattering (Mibémol; this work), depolarized light scattering [20], and dielectric loss [9,22,23]. The absolute scale is chosen arbitrarily (but temperature-independent) to make the data approximately coincide in the low-temperature, low-frequency corner, where they possibly reach a common asymptotic regime.

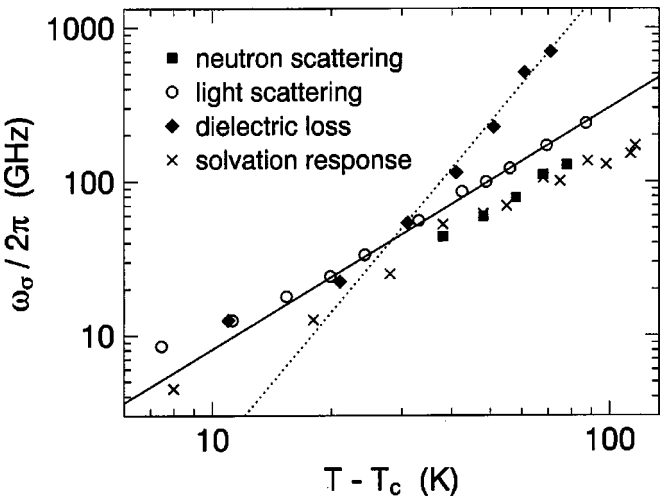

FIG. 14. Frequencies ω_σ, determined from MC fits with the same $\lambda = 0.72$, for neutron scattering, light scattering, dielectric loss, and solvation dynamics (from the time-domain analysis converted to $\omega_\sigma = 1/t_\sigma$). Temperatures are shown as $T - T_c$ with $T_c = 182$ K. The solid line shows the slope $1/2a = 1.572$ expected for the given value of λ; the dotted line, fitted to some dielectric data points, has a slope of 3.1 which is even steeper than the $1/2a + 1/2b = 2.4$ expected for the α-relaxation limit.

to any factorization property: there is no one temperature for which the measured $\epsilon''(\omega)$ and $\chi''(\omega)$ fall together; in particular, their minimum frequencies differ systematically.

At first sight, this outcome is a bad surprise, and could make us doubt whether fits of individual data sets with the asymptotic laws (3) and (4) are meaningful at all. On closer examination, the discrepancies between the three data sets can be traced back to two major differences: the individually different temperature ranges within which the β asymptote applies, and to a systematic shift in the frequency scale ω_σ.

B. Temperature range of β relaxation

Within idealized MC theory, all dynamic observables converge toward the same scaling limits (3) and (4), characterized by just one line shape parameter λ and one frequency scale ω_σ. This universality, however, is restricted to the lowest-order asymptote and does not imply a universal radius of convergence: the next-to-leading-order corrections already depend on the microscopic coupling [11], so that different observables may reach the asymptote at different temperatures and frequencies.

Nevertheless, for neutron and light scattering, as well as for solvation response, Eqs. (3) and (4) hold over rather large temperature intervals. In neutron scattering, Eq. (4) holds best between 220 and 260 K; at 210 K, the susceptibility minimum approaches the instrumental resolution function, and the signal becomes very weak: these technical limitations prevent us from following $S(q,\omega)$ closer to T_c. For light scattering, Fig. 8 confirms Eq. (4) with reasonable precision up to nearly 1.5 T_c.

On the other hand, the α master curve in Fig. 11 suggests that the range of β scaling is rather small for dielectric loss. This is corroborated by Fig. 14, in which ω_σ's from fits with fixed $\lambda = 0.72$ are compiled. For the lowest temperatures 193–213 K, the minima of $\epsilon''(\omega)$ coincide with the light scattering data, whereas for higher temperatures the dielectric ω_σ cross over to a much steeper temperature dependence characteristic for α relaxation (actually even steeper than the MC prediction $|\sigma|^{1/2a+1/2b}$).

C. Frequency scales ω_σ

As Fig. 14 shows, the ω_σ from neutron scattering fall about 35% below the ω_σ from light scattering. The good agreement of ω_σ from neutron scattering with t_σ^{-1} from solvation dynamics excludes the possibility that the discrepancy between neutron and light scattering lies only in multiple scattering or other technical shortcomings of neutron scattering. Ergo, at least one of the two scattering techniques does not see the true β asymptote of MC theory. On the other hand, the observed scaling, the quality of the g_λ fits, and the accord of the λ and T_c call for a MC interpretation, and indicate a transient behavior that is closely coupled to the universal β asymptote.

VI. DISCUSSION

A. Strength of α relaxation

Although there is no universal criterion for the validity of β scaling, an upper limit may be given: it is plausible that the asymptote [Eq. (3)] which is based on an expansion around the susceptibility minimum will no longer apply when the minimum ceases to exist. This happens when the height of the minimum, χ_σ, becomes comparable to the maximum of $\chi''(\omega)$ in the vibrational band. This condition also determines the highest temperature for which the proportionality (4) can hold.

On the other hand, the temperature where the susceptibility minimum disappears depends on the strength of the α peak. To explain this relation, we refer back to the α master plot in Fig. 11. Besides the dielectric $\epsilon''(\omega/\omega_{\max})$, the figure also shows $\chi''_{\mathrm{VH}}(\omega/\omega_{\max})$ from depolarized light scattering. For both data sets, the same frequency scale $\omega_{\max}$ has been applied, as determined from the maximum position of the dielectric α peak. The intensity scale of the light scattering data is arbitrary and has been adjusted by a global factor so that the maximum of the microscopic excitations has about the same height as for the dielectric data which are measured in absolute units.

Compared to the high-frequency maximum, the α peak is about four times weaker in light scattering than in dielectric loss. In the high-frequency wing, at, say, $\omega \simeq 30\omega_{\max}$, the ratio is reduced to a factor of about 2. This reduction is due to different positions of the α maxima, and to different slopes of the wings.

At still higher frequencies, the susceptibilities cross over toward the minimum. For the lowest temperatures shown in the figure, the ratio of 2 between dielectric and light scattering data survives in this frequency range. Thus, for a low-temperature value of σ, the β amplitude χ_σ for light scattering is about two times smaller than for dielectric loss.

Toward high temperatures, the range of β scaling ends for both techniques at about the same absolute value of χ_σ. Using the proportionality $\chi_\sigma \propto |\sigma|^{1/2}$, the dielectric data reach this limit after a temperature change four times smaller than the light scattering data require. Thus the strength of α re-

laxation can explain why the β scaling regime extends over only 30 K in dielectric loss, compared to 90 K or more in light scattering.

B. Frequency range of β relaxation

One can imagine many experimental imperfections that distort spectra measured in a scattering experiment. For instance, multiple scattering could overlay $S(q,\omega)$ with a convolution with itself. But any such distortions would affect the wings of the susceptibility much more than the region around the minimum. In particular, convolutions lead to similar corrections as intrinsic next-to-leading-order terms. Therefore, it is not easy to explain the discrepancy observed in ω_σ.

We note, however, that g_λ fits to the neutron scattering data in Fig. 4 extend up to frequencies between 200 and 400 GHz, whereas, in light scattering, the fitted g_λ already deviate from the measured susceptibilities a little above 100 GHz. It is therefore quite possible that our neutron scattering analysis sees a preasymptotic transient rather than the true g_λ.

This would resemble the situation in glycerol [39], where the $\chi''(\omega)$ allowed for the construction of a master curve and followed some MC predictions, although the full β asymptote was not reached. Numeric solutions of a simple two-correlator model showed how such a scenario can arise from a MC ansatz [40]. Similar fits, with one slave correlator for each observable, also work for propylene carbonate [41].

C. Current theoretical developments

Some of the questions raised by our experiments are also addressed by recent numerical solutions of MC equations and molecular-dynamics simulations. A MC analysis of the hard-sphere liquid as a function of wave number has demonstrated that corrections to scaling are of differing importance for different observables. Analytic expansions have shown that corrections to the α process are of higher order than corrections to the β asymptote: this may explain why α scaling holds over a wider range than the factorization property of β relaxation [11,12].

In a molecular-dynamics simulation of a liquid made of rigid diatomic molecules [42], orientational correlation functions have been analyzed for different angular momenta $l=0,1,2,\ldots$. All correlators were found to fulfil the MC factorization—with the pronounced exception of $l=1$, for which the position of the susceptibility minimum is shifted by a factor of 10. Although other results of the simulation do not even qualitatively agree with our PC data, they illustrate at least the possible importance of l-dependent corrections to scaling. A different scenario with an underlying type A transition for odd l was proposed recently [43].

It was noted before that the dielectric response couples only weakly to vibrational excitations [7], and the peculiar strength of the α peak in the $l=1$ correlator was also found in an analytic extension of MC theory to nonspherical particles [13]. A decomposition according to angular momenta might also explain the excellent accord between neutron scattering and solvation response found in Fig. 14, since both techniques see $l=0$, whereas light scattering might be dominated by $l=2$ [44].

D. Epilog

Earlier experiments on the β scaling regime in molecular liquids were described as ''tests'' of MC theory. In the meantime, more direct tests of the theory were performed in the simple spherical systems it is made for: the accuracy of experiments [15] and simulations [45] is impressive, and the accord with theory convincing.

In contrast, a MC theory of propylene carbonate does not exist. The treatment of linear molecules [13,14,46] provides an idea of how difficult it will be to formulate and solve a MC theory of realistic molecules.

But even without knowing exactly how such a theory will look, the basic structure of the MC approach suggests that the factorization of β relaxation will survive the inclusion of any innermolecular degree of freedom. In this sense, asymptotes (3) and (4) are indeed testable predictions.

However, experimental tests of these predictions do not automatically lead to clearcut conclusions about the validity of MC ideas. The observation of asymptotic scaling in a given data set does not yet guarantee a consistent MC interpretation, and conversely, failure to attain the asymptotes is not sufficient to exclude such an interpretation.

As summarized in Table I, more than ten MC fits of propylene carbonate have been reported, each of them successful, if judged separately. Only by comparing the freely adjusted parameters have we seen that not all of these fits represent the universal asymptote.

On the other hand, under conditions relevant for experiment even numeric solutions of MC do not necessarily reach the analytical asymptotes [11]. By derivation, these asymptotes are subject to several restrictions, and it is quite possible that some observables never attain the universal β regime.

On this background, the relevance of MC will not be decided by simplistic ''verification'' or ''falsification'': for the really interesting questions there exists no ready-to-use methodology [47]. The argumentation will become even more involved when experiments are compared to a few-correlator model that can be seen as a parametrization of the as-yet-nonexistent MC theory of molecular liquids [41]. Once we have acknowledged that experiments will never produce more than gradual evidence for or against MC theory, the frame is set within which our work can be summarized as a major breakthrough in the application of MC to molecular liquids.

Four different probes of fast dynamics have been given a simultaneous, consistent MC interpretation. After imposing one parameter λ, the other, T_c, is found to be reproducible within the precision of experimental temperature control. Differences in the β-relaxation asymptote are correlated with the tensorial character of the different observables, and the different extension of the scaling regime can be explained semiquantitatively in terms of α-relaxation strength. Such achievements do not only support MC theory as a useful tool for fitting and classifying experimental data—more importantly, by indicating that viscous flow in molecular liquids is governed by very much the same interplay of slow relaxation channels as in the simplest hard-sphere model, they confirm a progress in understanding.

ACKNOWLEDGMENTS

We thank H. Z. Cummins, M. Diehl, J. K. Krüger, H. Leyser, J. R. Sandercock, A. P. Sokolov, and J. Wiedersich for invaluable advice in setting up our Perot-Fabry spectrometer. We are grateful to W. Petry for continuous support, and we thank him as well as M. Fuchs, W. Götze, A. P. Singh, and T. Voigtmann for fruitful discussions. We also thank W. Götze for critically reading several versions of the manuscript. We acknowledge financial aid from the Bundes ministerium für Bildung, Wissenschaft, Forschung und Technologie through Verbundprojekte 03PE4TUM9 and 03LO5AU28 and through Contract No. 13N6917, from the Deutsche Forschungsgemeinschaft under Grant No. LO264/8–1, from the European Commission through Human Capital and Mobility Program ERB CHGECT 920001, and from the National Science Foundation under Grant No. CHE9809719. The Laboratoire Léon Brillouin is a laboratoire commun CEA–CNRS.

[1] W. Götze, in *Liquids, Freezing and the Glass Transition*, edited by J. P. Hansen, D. Levesque and D. Zinn-Justin (North Holland, Amsterdam, 1991).
[2] For a recent update and references to original work on MC theory, see Ref. [11].
[3] W. Götze and L. Sjögren, Rep. Prog. Phys. **55**, 241 (1992).
[4] W. Götze, J. Phys.: Condens. Matter **11**, A1 (1999).
[5] H.Z. Cummins *et al.*, Transp. Theory Stat. Phys. **24**, 981 (1995).
[6] W. Petry and J. Wuttke, Transp. Theory Stat. Phys. **24**, 1075 (1995).
[7] P. Lunkenheimer *et al.*, Phys. Rev. Lett. **77**, 318 (1996).
[8] P. Lunkenheimer, A. Pimenov, and A. Loidl, Phys. Rev. Lett. **78**, 2995 (1997).
[9] P. Lunkenheimer *et al.*, Prog. Theor. Phys. Suppl. **126**, 123 (1997).
[10] U. Schneider, P. Lunkenheimer, R. Brand and A. Loidl, J. Non-Cryst. Solids **235-237**, 173 (1998).
[11] T. Franosch *et al.*, Phys. Rev. E **55**, 7153 (1997).
[12] M. Fuchs, W. Götze and M.R. Mayr, Phys. Rev. E **58**, 3384 (1998).
[13] R. Schilling and T. Scheidsteger, Phys. Rev. E **56**, 2932 (1997).
[14] T. Franosch *et al.*, Phys. Rev. E **56**, 5659 (1997).
[15] W. van Megen and S.M. Underwood, Phys. Rev. E **49**, 4206 (1994).
[16] W. Götze and L. Sjögren, Z. Phys. B: Condens. Matter **65**, 415 (1987).
[17] W. Götze, J. Phys.: Condens. Matter **2**, 8485 (1990).
[18] L. Börjesson and W.S. Howells, J. Non-Cryst. Solids **131**, 53 (1991).
[19] M. Elmroth, L. Börjesson and L.M. Torell, Phys. Rev. Lett. **68**, 79 (1992).
[20] W.M. Du *et al.*, Phys. Rev. E **49**, 2192 (1994).
[21] E. Bartsch *et al.*, Ber. Bunsenges. Phys. Chem. **93**, 1252 (1989).
[22] P. Lunkenheimer *et al.*, Am. Chem. Soc. Symp. Ser. **676**, 168 (1996).
[23] U. Schneider, P. Lunkenheimer, R. Brand, and A. Loidl, Phys. Rev. E **59**, 6924 (1999).
[24] J. Ma, D. Vanden Bout, and M. Berg, J. Chem. Phys. **103**, 9146 (1995).
[25] J. Ma, D. Vanden Bout and M. Berg, Phys. Rev. E **54**, 2786 (1996).
[26] J. Wuttke, Physica B **266**, 112 (1999).
[27] G. Placzek, Phys. Rev. **93**, 895 (1954).
[28] J. Wuttke *et al.*, Z. Phys. B: Condens. Matter **91**, 357 (1993).
[29] M. Kiebel *et al.*, Phys. Rev. B **45**, 10301 (1992).
[30] M. Goldammer *et al.* (unpublished).
[31] S. Cusack and W. Doster, Biophys. J. **58**, 243 (1990).
[32] J. Wuttke (unpublished).
[33] The cross section for slow neutrons in ^{3}He is inverse proportional to the speed of the neutron. For economic reasons, the ^{3}He pressure and detector diameter are chosen such that the detection efficiency is high, but not close to 1. Therefore, the probability of detecting a scattered neutron depends on its energy. This energy dependence is regularly corrected for by standard formulas which in turn depend on very rough approximations for the detector geometry. Improvement will only be possible by direct experimentation on selected detector tubes.
[34] M. Fuchs, W. Götze, and A. Latz, Chem. Phys. **149**, 209 (1990).
[35] N.V. Surovtsev *et al.*, Phys. Rev. B **58**, 14 888 (1998).
[36] H.C. Barshilia, G. Li, G.Q. Shen, and H.Z. Cummins, Phys. Rev. E **59**, 5625 (1999).
[37] Using the interpolation
$$\chi''(\omega)=\chi_{\min}[a(\omega/\omega_{\min})^{-b}+b(\omega/\omega_{\min})^{a}]/(a+b)$$
instead of the full series expansion of g_λ [17] that we employ in the present paper. For the interpretation of dielectric data, the small numeric difference between the two expressions has no importance.
[38] Data from Du *et al.* [20]. On the scale of this figure, slight distortions of light scattering spectra by insufficient band passing are negligible.
[39] J. Wuttke *et al.*, Phys. Rev. Lett. **72**, 3052 (1994).
[40] T. Franosch, W. Götze, M. Mayr, and A.P. Singh, Phys. Rev. E **55**, 3183 (1997).
[41] W. Götze and T. Voigtmann, Phys. Rev. E (to be published).
[42] S. Kämmerer, W. Kob, and R. Schilling, Phys. Rev. E **58**, 2141 (1998).
[43] A. P. Singh, Ph.D. thesis, Technische Universität München, 1999 (unpublished).
[44] M.J. Lebon *et al.*, Z. Phys. B: Condens. Matter **103**, 433 (1997).
[45] M. Nauroth and W. Kob, Phys. Rev. E **55**, 657 (1997).
[46] L. Fabbian *et al.*, Phys. Rev. E **58**, 7272 (1998).
[47] P. K. Feyerabend, *Wider den Methodenzwang* (Suhrkamp, Frankfurt, 1986); see, in particular, pp. 388–389.
[48] L. Börjesson, M. Elmroth, and L.M. Torell, Chem. Phys. **149**, 209 (1990).
[49] A. Bondeau and J. Huck, J. Phys. (Paris) **46**, 1717 (1985).